

Non-stationary neural network for stock return prediction

Steven Y. K. Wong*, Jennifer Chan†, Lamiae Azizi†, Richard Y. D. Xu*

March 8, 2022

Abstract

We consider the problem of neural network training in a time-varying context. Machine learning algorithms have excelled in problems that do not change over time. However, problems encountered in financial markets are often *non-stationary*. We propose the *online early stopping* algorithm and show that a neural network trained using this algorithm can track a function changing with unknown dynamics. We applied the proposed algorithm to the stock return prediction problem studied in Gu et al. (2019) and achieved mean rank correlation of 4.69 %, almost twice as high as the expanding window approach. We also show that prominent factors, such as the size effect and momentum, exhibit time varying stock return predictiveness.

Keywords— return prediction, deep learning, online learning, non-stationarity

1 Introduction

Deep learning has made significant advances across a wide range of applications, such as achieving human-like accuracy in image recognition tasks (Schroff et al., 2015) and machine translation (Sutskever et al., 2014). These applications can be

*Steven Wong and Richard Xu are with School of Electrical and Data Engineering, University of Technology Sydney, Australia. Corresponding email: steven.ykwong87@gmail.com.

†Jennifer Chan and Lamiae Azizi are with School of Mathematics and Statistics, University of Sydney, Australia.

considered as *stationary* problems where the function of interest does not change with time. In some domains the prediction problem is *non-stationary*, where the underlying relationships between input and output change over time (also known as *concept drift* in machine learning, Gama et al. 2014). Recently, Aydore et al. (2019) proposed the *Dynamic Exponentially Time-Smoothed Stochastic Gradient Descent* optimization algorithm (DTS-SGD) which allows a neural network to adapt to a non-stationary function. To the best of our knowledge, this is the first attempt at bridging the gap from deep learning to non-stationary problems.

The motivating application of our work is in predicting cross-sectional stock returns at time t using history up to $t - 1$. Literature has documented evidence of non-stationarity of the true asset pricing model. Bossaerts and Hillion (1999) studied the model selection problem in the context of predicting international stocks and found that models chosen by common statistical selection criteria fail to retain predictive power out of sample and is indicative of model non-stationarity. Pesaran and Timmermann (1995) documented similar findings in U.S. stocks. At every month, the authors performed linear regressions with permutations of regressors and compared both statistical and financial measures for model selection. Both predictability and regression coefficients of the selected model changed over time.

Machine learning in financial markets is still in its infancy. Weigand (2019) provided a recent survey of the state of machine learning applied to empirical finance and noted that literature is dominated by regression-based techniques. More recent works employed “gold standard” techniques, such as *dropouts* (Srivastava et al., 2014) and *batch normalization* (Ioffe and Szegedy, 2015), as well as *momentum* and *learning rate decay* in optimization (Kingma and Ba, 2015). Messmer (2017) performed a random search over hyperparameter space for the best neural network configuration for stock return prediction. The author found that the best network had 7 hidden layers, 78 hidden units¹, a low learning rate of just 10^{-5} , and achieved R^2 of 7.31 % vs. 4.5 % of linear regression in U.S. large and mid-cap stocks². Abe and Nakayama (2018) compared neural networks to Support Vector Machine and random forests in predicting one-month ahead Japanese stock returns. Performance metrics were rank correlation and directional accuracy, arguing that these are more relevant to investors. Batch size was set to the entire stock universe in each month. The best performing model (by rank correlation) had 8 hidden layers and achieved rank correlation of 5.82 %. Gu et al. (2019) compared several machine learning algorithms for predicting monthly returns of

¹The author did not provide the network topology. However, a network with 7 hidden layers and 78 hidden units would suggest a very narrow network.

²Note that the dependent variable in this paper is cross-sectionally ranked stock returns. Thus, R^2 from this paper are not comparable to those reported in Gu et al. (2019).

U.S. equities. The data set consists of all stocks listed on NYSE, AMEX and NASDAQ, with 94 firm characteristics, 74 sector dummy variables, as well as interaction terms with 8 macroeconomic indicators resulting in 920 features. The authors reported both tree-based algorithms and neural networks resulted in an improved R^2 of 0.27% and 0.4% respectively. Shallow networks outperformed deeper networks which the authors have attributed to the small data set and low signal-to-noise ratio. The best performing network had three hidden layers, with 32–16–8 nodes for each hidden layer respectively. This observation is particularly interesting. If stock returns are a result of complex interactions of factors then one would expect a deeper and/or wider network to perform well. Majority of the data set has been made available to the public.

To the best of our knowledge, this the first time a comprehensive U.S. equities feature set has been released, providing a rich source of relatively untapped data for machine learning research. For this reason, the work of Gu et al. (2019) forms the basis of this paper. Our contributions in this paper are as follows:

- We propose the *online early stopping* algorithm which allows the network to track a time-varying function. We achieved mean rank correlation of 4.69% on the U.S. equities data set, compared to 2.44% under an expanding window approach³ studied in Gu et al. (2019). This algorithm can be applied to an existing network and requires significantly less time to train than the setup used in Gu et al. (2019).
- We show that features exhibit time-varying importance and that the true model changed over time. We find that certain features, such as market capitalization (the size effect) faded in importance over time. This highlights the importance to have a non-stationary model.
- We provide an alternative viewpoint to the shallow–deep learning debate. Our analysis suggests only a small set of features contributed to predictive performance. This may be due to most features lacking in predictive power, or features are correlated and L1 regularization has encouraged the network to only use a subset. This would likely lead to a simpler network.

In the rest of this paper, we denote our replication of Gu et al. (2019) as *DNN* (Deep Neural Network) and Online Early Stopping as *OES*. This paper is organized as follows. In Section 2, we define our problem and survey existing works on our cross-disciplinary problem, covering online optimization and deep learning. Section 3 outlines our main contribution of this paper — an online

³In this paper, we will use the *pooled* approach and the *expanding window* approach interchangeably.

early stopping algorithm which introduces non-stationarity to a neural network and is an improvement over DTS-SGD. Data and experimental setup is outlined in Section 4 and results are presented in Section 5. Finally, we provide a discussion on the empirical finance problem and future works.

2 Preliminaries

2.1 Definitions

We denote vectors with bold lower-case letters and matrices with bold upper-case letters. The i -th stock at time $t = 1, \dots, T$ in vector \mathbf{v}_t is $v_{t,i}$. To simplify notations, we define return of stock i as return over next period, i.e., $r_{t,i} = (p_{t+1,i} + d_{t+1,i})/p_{t,i} - 1$, where $p_{t,i}$ is price at time t and $d_{t,i}$ is dividend at t if a dividend is paid, and zero otherwise.

Similar to a classical online learning setup, an investor iteratively makes portfolio allocation decisions at each time period. We call this iterative process *per interval training*. There are n stocks in the market, each with m characteristics and forming input matrix $\mathbf{X}_t \in \mathbb{R}^{n \times m}$ at time t . The i -th row in \mathbf{X}_t is feature vector \mathbf{x}_i of stock i . Investor predicts stock returns $\hat{\mathbf{r}}_t \in \mathbb{R}^n$ by choosing $\boldsymbol{\theta}_t \in \Omega$, which parameterizes prediction function $F : \mathbb{R}^{m \times n} \mapsto \mathbb{R}^n$. Market reveals \mathbf{r}_t and, for regression purposes, investor incurs squared loss,

$$J_t(\boldsymbol{\theta}_t) = \frac{1}{n} \sum_{i=1}^n (r_{t,i} - F(\mathbf{x}_{t,i}; \boldsymbol{\theta}_t))^2.$$

We adopt the same customary assumptions in online optimization as Aydore et al. (2019):

- J_t is bounded: $|J_t| \leq D; D > 0$,
- J_t is L-Lipschitz: $|J_t(\mathbf{a}) - J_t(\mathbf{b})| \leq L \|\mathbf{a} - \mathbf{b}\|; L > 0$,
- J_t is β -smooth: $\|\nabla J_t(\mathbf{a}) - \nabla J_t(\mathbf{b})\| \leq \beta \|\mathbf{a} - \mathbf{b}\|$.

We denote the gradient of J_t at $\boldsymbol{\theta}_t$ as $\nabla J_t(\boldsymbol{\theta}_t)$ and stochastic gradient as $\hat{\nabla} J_t(\boldsymbol{\theta}_t) = \mathbb{E}[\nabla J_t(\boldsymbol{\theta}_t)]$, or where the context is obvious, ∇_t and $\hat{\nabla}_t$ respectively.

The true function $\phi_t : \mathbb{R}^{n \times m} \mapsto \mathbb{R}^n$ drifts over time and is approximated by F with time-varying $\boldsymbol{\theta}_t$. Investor's objective is to minimize loss incurred by choosing the best $\boldsymbol{\theta}_t$ at time t using observed history up to $t-1$. Both the function form and time-varying dynamics of ϕ are not known. Hence a neural network is used to model the cross sectional relationship at each t and the non-stationarity is formulated as a network weights tracking problem.

In the simplest sense, a fully connected neural network consists of an input layer, one or more hidden layers, and an output layer. The output of each layer acts as input to the next layer and loss is “backpropagated” by taking the partial derivative of loss w.r.t. weights. Each layer consists of activation function f (i.e., *rectified linear unit*), weights ω , bias b , and output $f(\mathbf{x}; \omega, b) = f(\mathbf{x}^T \omega + b)$. The i -th layer of the network is denoted as $f^{(i)}$. For brevity, we drop the layer designation, and denote the entire network as F and weight vector set $\theta = \bigcup_{i=1}^{\ell} \{\omega^{(i)}, b^{(i)}\}$, where ℓ is the number of layers. The network is trained with *stochastic gradient descent* (or variants),

$$\theta_{k+1} = \theta_k - \eta \hat{\nabla} J_t(\theta_k),$$

where θ_k is the weight vector at optimization iteration⁴ k and η is step size. At time period t , τ_t denotes the number of optimization iterations that was used to train the network. Interested readers are referred to the text by Goodfellow et al. (2016) for a comprehensive review of neural networks.

2.2 Early stopping in neural network training

High learning capacity models such as neural networks can often overfit. Optimization can be terminated early based on some stopping criteria determined using a validation data set. This procedure is called *early stopping*. An effective stopping criteria is to monitor loss on validation set (Morgan and Bourlard, 1990; Reed, 1993; Prechelt, 1998; Mahsereci et al., 2017), where a portion of available data is reserved for validation. Training is stopped when validation loss decreases by less than a predefined amount. Algorithm 1 contains the schematics of an early stopping algorithm with one modification and was adapted from Algorithm 7.1 and Algorithm 7.2 in Goodfellow et al. (2016). Validation is performed before the first training step to allow for the case where $\tau' = 0$ (i.e., we start from the optimal weights).

Early stopping can be seen as a regularization technique that limits the optimizer to search in the parameter space near the starting parameters (Sjberg and Ljung, 1995; Goodfellow et al., 2016). In particular, given optimization steps τ , the product $\eta\tau$ can be interpreted as the effective capacity which bounds reachable parameter space from θ_0 , thus behaving like L_2 regularization (Goodfellow et al., 2016).

For time series problems where chronological ordering is important, popular approaches include expanding window and rolling window where each time slice within the rolling window is pooled (Rossi and Inoue, 2012). Instead of randomly

⁴Also called *epochs*.

Algorithm 1 Early stopping procedure

Require: Maximum iterations $\{\mathcal{T} \in \mathbb{N} | \mathcal{T} > 0\}$; tolerance $\{\varepsilon \in \mathbb{R} | \varepsilon > 0\}$;
patience $\{Q \in \mathbb{N} | Q > 0\}$

1: **function** EARLYSTOPPING($\boldsymbol{\theta}, \mathbf{X}_{train}, \mathbf{r}_{train}, \mathbf{X}_{test}, \mathbf{r}_{test}$)
2: $\boldsymbol{\theta}_{best} \leftarrow \boldsymbol{\theta}$
3: $q \leftarrow 0$
4: $J_{best} \leftarrow J(\mathbf{r}_{test}, F(\mathbf{X}_{test}; \boldsymbol{\theta}))$
5: **for** $i = 1, \dots, \mathcal{T}$ **do**
6: $\boldsymbol{\theta} \leftarrow \boldsymbol{\theta} - \eta \hat{\nabla} J(\mathbf{r}_{train}, F(\mathbf{X}_{train}; \boldsymbol{\theta}))$
7: $J' \leftarrow J(\mathbf{r}_{test}, F(\mathbf{X}_{test}; \boldsymbol{\theta}))$
8: **if** $J' < J_{best}$ **then**
9: $\tau_{best} \leftarrow i$
10: $\boldsymbol{\theta}_{best} \leftarrow \boldsymbol{\theta}$
11: $J_{best} \leftarrow J'$
12: **end if**
13: **if** J' did not improve by at least ε **then**
14: $q \leftarrow q + 1$
15: **if** $q \geq Q$ **then**
16: **break** ▷ Assume convergence
17: **end if**
18: **else**
19: $q \leftarrow 0$
20: **end if**
21: **end for**
22: **return** $\tau_{best}, \boldsymbol{\theta}_{best}$
23: **end function**

splitting training and test sets, the *out-of-sample* procedure⁵ can be used where the end of the series is withheld for evaluation. This is unsatisfactory for two reasons. First, each time period is drawn from a different data distribution \mathcal{D} (hereon denoted as \mathcal{D}_t for data set drawn at time t). A pooled regression with window size k effectively assumes data at $t+1$ is drawn from $\frac{1}{k} \sum_{j=0}^{k-1} \mathcal{D}_{t-j}$. Secondly, if data is scarce in terms of time periods (for instance, monthly data with a window size of 12 months), estimates for optimal optimization steps $\hat{\tau}$ can have large stochastic error. To the best of our knowledge, there is no procedure for adapting early stopping to be used in an online and time-varying context.

2.3 Online optimization

Optimizing network weights to track a function evolving under unknown dynamics is an online optimization problem. A discussion on relevant concepts in online optimization is provided. Interested readers are encouraged to read the text by Shalev-Shwartz (2012) for an introduction. In this section, iterate $\boldsymbol{\theta}$ and loss function J share the same contextual meaning as the rest of this paper. We abuse notations by using the same symbols.

In online convex optimization, a player iteratively chooses iterate $\boldsymbol{\theta}_t \in \Omega$, where Ω is a set of admissible iterates⁶. Nature reveals potentially adversarial loss function $J_t \in \mathcal{K}$ and player incurs loss $J_t(\boldsymbol{\theta}_t)$, where \mathcal{K} is a convex set of loss functions. The most basic performance measure of an online learning algorithm is the *average regret* (also called *static regret*), defined as the difference in average loss between the player and the *best fixed optimum in hindsight*. More formally,

$$\mathcal{R}_T^s = \sum_{t=1}^T J_t(\boldsymbol{\theta}_t) - \min_{\boldsymbol{\theta}^*} \sum_{t=1}^T J_t(\boldsymbol{\theta}^*),$$

where $\boldsymbol{\theta}^*$ is the best minimizer. The goal is to design algorithms that minimize \mathcal{R}_T^s , a cumulative deficit against the best minimizer. One of the simplest online learning algorithm for static regret is the *Follow-the-Leader* algorithm (Kalai and Vempala, 2005; Shalev-Shwartz, 2012), defined as,

$$\boldsymbol{\theta}_t = \arg \min_{\boldsymbol{\theta} \in \Omega} \sum_{i=1}^{t-1} J_i(\boldsymbol{\theta}).$$

⁵As described in Bergmeir et al. (2018).

⁶In online optimization literature, iterate is often denoted as x_t and loss function as f . We have used $\boldsymbol{\theta}_t$ to be consistent with our parameter of interest and J to avoid conflict with our use of f .

At each round t , the algorithm simply elects the best minimizer in the data seen to date. This algorithm shares some resemblance to the expanding window training scheme used by Gu et al. (2019), where the model is re-trained on the entire data set at every interval and will converge to the best fixed optimum. There are two limitations with average regret: the distribution of loss functions J must be stationary, and J must be convex.

Recently, Hazan et al. (2017) extended online convex optimization to the non-convex stationary case. Non-convex optimization is NP-Hard⁷. Therefore, existing non-convex optimization algorithms focus on finding local minima (Hazan et al., 2017). Aydore et al. (2019) extended this work to the non-stationary case, proposing to measure performance with *dynamic local regret*,

$$DLR_w(T) = \sum_{t=1}^T \|\nabla S_{t,w,\alpha}(\boldsymbol{\theta}_t)\|^2,$$

where $S_{t,w,\alpha}(\boldsymbol{\theta}_t) = \frac{1}{W} \sum_{i=0}^{w-1} \alpha^i J_{t-i}(\boldsymbol{\theta}_{t-i})$ is the exponentially weighted history of loss functions, $W = \sum_{i=0}^{w-1} \alpha^i$ is the normalization factor, and $J_t(\boldsymbol{\theta}_t) = 0$ for $t \leq 0$. To minimize dynamic local regret, Aydore et al. (2019) proposed the *dynamic exponentially time-smoothed online gradient descent* algorithm, as presented in Algorithm 2. Note that weights are updated with the weighted sum of past gradients

Algorithm 2 Dynamic Exponentially Time-Smoothed Stochastic Gradient Descent (DTS-SGD), as detailed in Aydore et al. (2019).

Require: Window size $w \geq 1$, learning rate $\eta > 0$, exponential smoothing parameter $0 < \alpha < 1$, normalization parameter $W = \sum_{i=0}^{w-1} \alpha^i$, set $\theta_1 \in \Omega$ arbitrarily

- 1: **for** $t = 1, \dots, T$ **do**
- 2: Predict θ_t . Observe cost function J_t
- 3: Update $\theta_{t+1} = \theta_t - \frac{\eta}{W} \sum_{i=0}^{w-1} \alpha^i \hat{\nabla} J_{t-i}(\theta_{t-i})$
- 4: **end for**

$\hat{\nabla} J_{t-i}(\theta_{t-i})$, rather than $\hat{\nabla} J_{t-i}(\boldsymbol{\theta}_t)$.

In analyzing this algorithm, we note two potential weaknesses. Firstly, neural networks are notoriously difficult to train. Geometry of the loss function is plagued by the abundance of local minima and saddle points (see Chapter 8.2 of Goodfellow et al., 2016). Momentum and learning rate decay strategies (for instance, Sutskever et al., 2013; Kingma and Ba, 2015) have been introduced which requires multiple

⁷In computer science, NP-Hard refers a class of problems where no known polynomial run-time algorithm exists.

passes over training data, adjusting learning rate each time to better traverse the loss surface. DTS-SGD is a single weight update at each time period which may have difficulty traversing highly non-convex loss surfaces. Secondly, during our simulation tests, we observed that loss can increase after weight update. One possibility is that a past gradient is taking the weights further away from the current local minima. On our U.S. equities data set, we observed exploding gradient when using DTS-SGD and could not complete training.

3 Online early stopping

3.1 Calibration in online learning

In this section we present our main theoretical results. The motivating concept for dynamic local regret is *calibration* (Foster and Vohra, 1998; Aydore et al., 2019). Consider the first order Taylor series expansion of cumulative loss, where $\boldsymbol{\theta}_t$ is perturbed by \mathbf{u} (a small perturbation with the same shape as $\boldsymbol{\theta}$),

$$\sum_{t=1}^T J_t(\boldsymbol{\theta}_t + \mathbf{u}) \approx \sum_{t=1}^T J_t(\boldsymbol{\theta}_t) + \sum_{t=1}^T \langle \mathbf{u}, \nabla J_t(\boldsymbol{\theta}_t) \rangle,$$

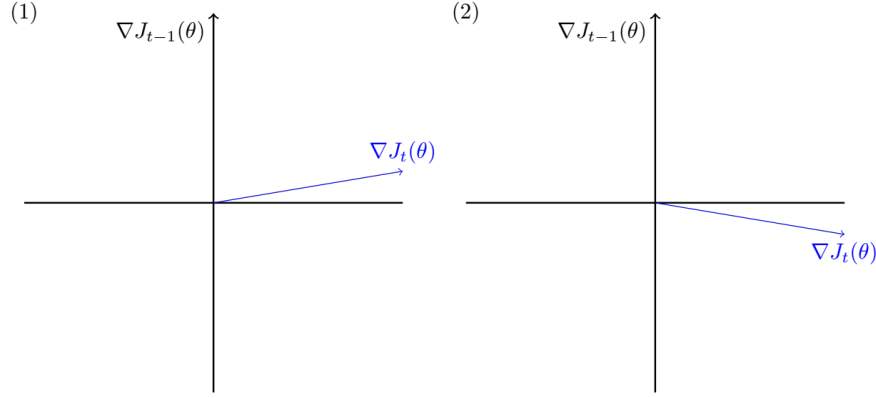
where $\langle \mathbf{a}, \mathbf{b} \rangle$ is inner product of \mathbf{a} and \mathbf{b} . If the series of updates $\{\boldsymbol{\theta}_1, \dots, \boldsymbol{\theta}_T\}$ are *well calibrated* w.r.t. $\{J_1, \dots, J_T\}$, then perturbing $\boldsymbol{\theta}_t$ by \mathbf{u} cannot substantially reduce cumulative loss (Aydore et al., 2019). A small shift in all $\boldsymbol{\theta}_t$ will have no net effect on total loss as increases in some intervals are offset by decreases in other intervals. This concept is the cornerstone of our proposed algorithm.

3.2 Online early stopping algorithm

Recall that in our setup, $\hat{\boldsymbol{\theta}}_t$ are weights trained on data up to $t-1$ for prediction on interval t , and J_t is not known at the time of prediction. Let $\boldsymbol{\theta}' = \boldsymbol{\theta}_{t-2}$ be our starting point of optimization, $\mathbf{g} = \nabla J_{t-1}(\boldsymbol{\theta}')$ and $\mathbf{g}' = \nabla J_t(\boldsymbol{\theta}')$. The possible scenarios during training are (also illustrated in Figure 1):

1. If $\left| \cos^{-1} \frac{[\langle \mathbf{g}, \mathbf{g}' \rangle]}{\|\mathbf{g}\| \|\mathbf{g}'\|} \right| < \pi/2$, then moving along \mathbf{g} will also improve $J_t(\boldsymbol{\theta}')$ until \mathbf{g} is perpendicular to \mathbf{g}' or $\boldsymbol{\theta}'$ has reached the local minima of J_{t-1} .
2. If $\left| \cos^{-1} \frac{[\langle \mathbf{g}, \mathbf{g}' \rangle]}{\|\mathbf{g}\| \|\mathbf{g}'\|} \right| \geq \pi/2$, then following \mathbf{g} will not improve $J_t(\boldsymbol{\theta}')$ and training should terminate.

Figure 1: As $\boldsymbol{\theta}$ move along the direction of \mathbf{g} , if the angle between \mathbf{g} and \mathbf{g}' are less than $\pi/2$ (left), then training will improve $J_t(\boldsymbol{\theta})$. If the angle is greater than $\pi/2$ (right), then training will not improve $J_t(\boldsymbol{\theta})$.



Our strategy is to modify the early stopping algorithm to recursively estimate $\hat{\tau}_t$ and is outlined in Algorithm 3. Let τ_t be the optimal number of optimization steps at time t and $\hat{\tau}_t$ be the estimated number of optimization steps. At iteration t , we solve,

$$\tau_{t-2} = \arg \min_{\tau' \geq 0} J_{t-1} \left[\boldsymbol{\theta}_{t-2} - \eta \sum_{i=1}^{\tau'} \hat{\nabla}_{t-2}(\boldsymbol{\theta}_{t-2,i}) \right], \quad (1)$$

using J_{t-1} as validation set. This leads to optimal weights trained on \mathcal{D}_{t-2} for prediction on \mathcal{D}_{t-1} ,

$$\boldsymbol{\theta}_{t-1} = \boldsymbol{\theta}_{t-2} - \eta \sum_{i=1}^{\tau_{t-2}} \hat{\nabla}_{t-2}(\boldsymbol{\theta}_{t-2,i}). \quad (2)$$

To make predictions on \mathcal{D}_t , we set $\hat{\tau}_{t-1} = \frac{1}{t-2} \sum_{i=1}^{t-2} \tau_i$ and train *prediction weights* on \mathcal{D}_{t-1} ,

$$\hat{\boldsymbol{\theta}}_t = \boldsymbol{\theta}_{t-1} - \eta \sum_{i=1}^{\hat{\tau}_{t-1}} \hat{\nabla}_{t-1}(\boldsymbol{\theta}_{t-1,i}). \quad (3)$$

Suppose $\boldsymbol{\theta}_t$ evolves under the dynamics of,

$$\boldsymbol{\theta}_t = \boldsymbol{\theta}_{t-1} - v_{t-1} \nabla J_{t-1}(\boldsymbol{\theta}_{t-1}), \quad (4)$$

where v_{t-1} is sampled from an unknown distribution. v_{t-1} should be interpreted as a scaling factor which provides the optimal prediction weights on \mathcal{D}_t , if we are restricted to traveling along the direction of $\nabla J_{t-1}(\boldsymbol{\theta}_{t-1})$. v_{t-1} can be approximated

by,

$$\mathbb{E}[v_{t-1}] = \hat{v}_{t-1} \approx \eta \hat{\tau}_{t-1}. \quad (5)$$

Thus, $\eta \hat{\tau}_{t-1}$ is a measure of variations between $\boldsymbol{\theta}_t$ and $\boldsymbol{\theta}_{t-1}$. Using our β -smooth assumption (in Section 2.1),

$$\left\| \nabla J_t(\boldsymbol{\theta}_t) - \nabla J_t(\hat{\boldsymbol{\theta}}_t) \right\| \leq \beta \left\| \boldsymbol{\theta}_t - \hat{\boldsymbol{\theta}}_t \right\| \quad (6)$$

$$\sum_{t=2}^T \left\| \nabla J_t(\boldsymbol{\theta}_t) - \nabla J_t(\hat{\boldsymbol{\theta}}_t) \right\| \leq \sum_{t=2}^T \beta \left\| \boldsymbol{\theta}_t - \hat{\boldsymbol{\theta}}_t \right\|, \quad (7)$$

where we start from $t = 2$ as our algorithm requires at least 2 observations. The elegance of Equation 7 is that it conforms with conventional notions of regret (for example, see the definition of dynamic regret in Yang et al., 2016), with cumulative loss replaced with cumulative gradient deficit against an optimal outcome. If v_t is sampled from a constant distribution Z , then $\mathbb{E} \left[\left\| \boldsymbol{\theta}_t - \hat{\boldsymbol{\theta}}_t \right\|^2 \right]$ measures variance of Z . In general, Equation 7 indicates that the sum of gradient deficit is proportional to variations of each consecutive $\boldsymbol{\theta}_t$. This concept is illustrated in Figure 2.

Algorithm 3 outlines the online early stopping procedure and consists of two steps: (i) recursively estimate optimal training steps τ' at $t - 1$ by training on \mathcal{D}_{t-2} and validating on \mathcal{D}_{t-1} ; (ii) train on \mathcal{D}_{t-1} for $\hat{\tau}$ steps. *EarlyStopping* on line 3 is outlined in Algorithm 1. At each iteration, two trailing intervals of data are used to train $\boldsymbol{\theta}$. On line 3, optimal weights at $t - 2$ (or randomly initialized if $t = 2$) is trained on $\mathbf{X}_{t-2}, \mathbf{r}_{t-2} \sim \mathcal{D}_{t-2}$ and validated on $\mathbf{X}_{t-1}, \mathbf{r}_{t-1} \sim \mathcal{D}_{t-1}$ (line 3) which rolls $\boldsymbol{\theta}_{t-2}$ forward by one period. The network is then trained on $\mathbf{X}_{t-1}, \mathbf{r}_{t-1} \sim \mathcal{D}_{t-1}$ by $\hat{\tau}$ iterations. At this point, $\boldsymbol{\theta}$ represents the best estimated weights $\hat{\boldsymbol{\theta}}_{t|t-1}$ and is ready to be used for predictions. At the next iteration, we start from $\boldsymbol{\theta}_{t-2}$ (which has been validated against \mathcal{D}_{t-2}) in order to estimate τ' for $t - 1$.

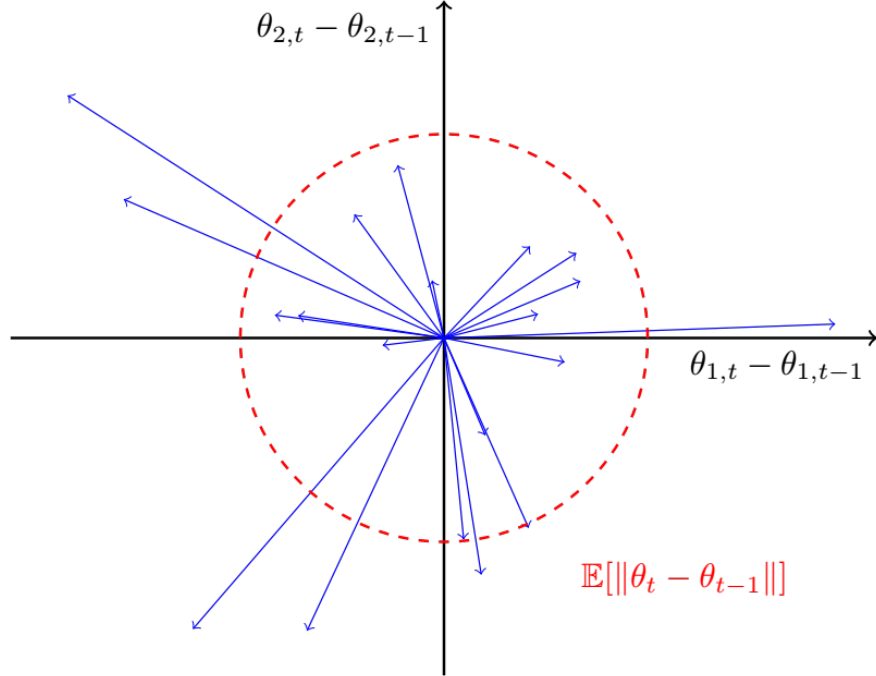
4 Data

In this work, we conduct two empirical studies. First is based on simulation data which highlights the use case of online early stopping, and the second on predicting U.S. stock returns based on the data set in Gu et al. (2019).

4.1 Simulation

To illustrate the use case of online early stopping, we have created the following synthetic data set.

Figure 2: Illustration of estimating $\mathbb{E} [\|\boldsymbol{\theta}_t - \boldsymbol{\theta}_{t-1}\|]$. Suppose $\boldsymbol{\theta}_t = [\theta_{1,t} \quad \theta_{2,t}]$ is a row vector with two elements. Twenty one random $\boldsymbol{\theta}_t$ vectors were drawn with each $\boldsymbol{\theta}_t - \boldsymbol{\theta}_{t-1}$ pair represented as an arrow. The circle has radius $\frac{1}{20} \sum_{t=2}^{21} \|\boldsymbol{\theta}_t - \boldsymbol{\theta}_{t-1}\|$. $\hat{\boldsymbol{\theta}}_t$ is regularized by limiting how far it can travel from $\boldsymbol{\theta}_{t-1}$ which is $\mathbb{E} [\|\boldsymbol{\theta}_t - \boldsymbol{\theta}_{t-1}\|]$.



- $T = 180$ months, each month consists of $n = 200$ observations.
- Each observation has $m = 100$ features, forming input matrix of $\mathbf{X} \in \mathbb{R}^{180 \times 200 \times 100}$ and output vector $\mathbf{r} \in \mathbb{R}^{180 \times 200}$.
- Let $x_{t,i,j}$ be the value of feature j of stock i at time t . Each feature value is randomly set to $x_{t,i,j} \sim N(0, 1)$.
- Each feature has latent relationship $v_{t,j} = 0.95v_{t-1,j} + 0.05\delta_{t,j}$, where $\delta_{t,j} \sim N(0, 1)$ and $v_{0,j} \sim N(0, 1)$. Latent relationship follows a Wiener process and drifts over time.
- Each output value is $r_{t,i} = \sum_{j=1}^m \tanh(x_{t,i,j} \times v_{t,j}) + \epsilon_{t,i}$, where $\epsilon_{t,i} \sim N(0, 1)$. Thus, \mathbf{r}_t is non-linear w.r.t. \mathbf{X}_t and the relationship changes over time.

Algorithm 3 General framework for online early stopping. The outer loop recursively estimates $\hat{\tau}$.

Require: data $\mathbf{X}_t, \mathbf{r}_t \sim p_t$ at interval t ; $\boldsymbol{\theta}_0$ initialized randomly

```

1:  $\tau' \leftarrow 0$ 
2: for  $t = 2, \dots, T$  do
3:    $\tau', \boldsymbol{\theta}_{t-1} \leftarrow \text{EARLYSTOPPING}(\boldsymbol{\theta}_{t-2}, \mathbf{X}_{t-2}, \mathbf{r}_{t-2}, \mathbf{X}_{t-1}, \mathbf{r}_{t-1})$ 
4:    $\hat{\tau} \leftarrow \frac{\hat{\tau}(t-2) + \tau'}{t-1}$ 
5:    $\boldsymbol{\theta} \leftarrow \boldsymbol{\theta}_{t-1}$ 
6:   for  $i = 1, \dots, \lfloor \hat{\tau} + 0.5 \rfloor$  do
7:      $\boldsymbol{\theta} \leftarrow \boldsymbol{\theta} - \eta \hat{\nabla}_{t-1}(\boldsymbol{\theta})$ 
8:   end for
9:    $\hat{\theta}_t \leftarrow \boldsymbol{\theta}$ 
10:  Receive input  $\mathbf{X}_t$ 
11:  Predict  $\hat{\mathbf{r}}_t \leftarrow F(\mathbf{X}_t; \hat{\theta}_t)$ 
12:  Receive output  $\mathbf{r}_t$ 
13: end for

```

We have used the same network setup as Section 4.2 (outlined in Table 1) but with a batch size of 50. DNN was re-fitted at every 10-th intervals. Hyperparameters for OES were chosen using the first 60 intervals as training data and next 60 intervals as validation data. Out-of-sample performance was calculated on the remaining 60. DTS-SGD follows the same training scheme as OES, with additional hyperparameters: $W \in \{5, 10, 20\}$, $\alpha \in \{0.9, 0.8, 0.7\}$.

4.2 Model and U.S. equities data

The U.S. equities data set in Gu et al. (2019) consists of all stocks listed in NYSE, AMEX, and NASDAQ from March 1957 to December 2016. Average number of stocks exceeds 5,200. Excess returns are calculated as forward one month stock returns over Treasury-bill rates. Covariates include 94 firm level features, 74 industry dummy variables (based on first two digits of SIC code) and interaction terms with 8 macroeconomic indicators. Firm level characteristics include share price based measures, valuation metrics and accounting ratios. The purpose of interacting firm level characteristics with macroeconomic indicators is to capture any time-varying dynamics that are related to (common across all stocks) macroeconomic indicators. For instance, suppose valuation metrics have a stronger relationship with stock returns during periods of high inflation. Then, this information will be encoded in the interaction term. The aggregated data set therefore contains

$94 \times (8 + 1) + 74 = 920$ features. Each feature has been appropriately lagged to avoid look-forward bias, and are cross-sectionally ranked and scaled to $[-1, 1]$. Table A.6 in Gu et al. (2019) contains the full list of firm characteristics.

A subset of the data is available on Dacheng Xiu’s website⁸ which contains 94 firms level characteristics and 74 industry classification. Our main result uses $94 + 74 = 168$ firm level features but results with the full 920 features are also provided as a comparison. At this point, it is useful to remind readers that our goal is to track a non-stationary function when time-varying dynamics are unknown. In other words, we assume that time-varying dynamics between stock returns and features are not well understood or are unobservable. As such, the subset of data without interaction terms is sufficient for our problem. If macroeconomic indicators do encode time-varying dynamics, our network will track changing macroeconomic conditions automatically.

Data is divided into 18 years of training (from 1957 to 1974), 12 years of validation (1975-1986), and 30 years of out-of-sample tests (1987-2016). Training and validation sets are rolled forward by 12 months at the end of every December and the model is re-fitted. We use monthly total returns of individual stocks from CRSP. Where stock price is unavailable at the end of month, we use the last available price during the month. Table 1 records test configurations as outlined in Gu et al. (2019) and in our replication. A total of six hyperparameter combinations were tested. Batch size of 1,000 for OES was chosen arbitrarily.

To train OES, we have kept the first 18 years (to 1974) as training data and next 12 years (to 1986) as validation data. For each permutation of hyperparameter set, we have trained an online learner up to 1986. Hyperparameter search is only performed on this period, as opposed to every year in Gu et al. (2019). As the algorithm does not depend on a separate set of data for validation, we simply take the hyperparameter set with the lowest monthly average MSE over 1975-1986 as the best configuration to use for rest of the data set.

5 Empirical results

5.1 Performance metrics

As outlined in Section 2.1, our problem is based on an investor making iterative portfolio allocation decisions. Gu et al. (2019) used pooled R_{oos}^2 without de-meaning as the main performance metric,

$$R_{oos}^2 = 1 - \frac{\sum_{(t,i) \in \mathcal{D}_{oos}} (r_{t,i} - \hat{r}_{t,i})^2}{\sum_{(t,i) \in \mathcal{D}_{oos}} r_{t,i}^2},$$

⁸Dacheng Xiu’s website <https://dachxiu.chicagobooth.edu/>

Table 1: Disclosed model parameters in Gu et al. (2019) and in our replication. We have filled missing values with the cross-sectional median or zero if median is unavailable. “H” is hidden layer activation. “O” is output layer activation.

Parameter	Gu et al. (2019)	This paper
Preprocessing	Rank [-1, 1]; Fill median	Rank [-1, 1]; Fill median/0
Hidden layers	32-16-8	32-16-8
Activation	H: ReLU / O: Linear	H: ReLU / O: Linear
Batch size	10,000	DNN 10,000 / OES 1,000
Batch normalization	Yes	Yes
l_1 penalty	$[10^{-5}, 10^{-3}]$	$\{10^{-5}, 10^{-4}, 10^{-3}\}$
Early stopping	Patience 5	Patience 5 / Tolerance 0.001
Learning rate	$[0.001, 0.01]$	$\{0.001, 0.01\}$
Optimizer	ADAM	ADAM
Loss function	MSE	MSE
Ensemble	Average over 10	Average over 10

where \mathcal{D}_{oos} is the pooled out-of-sample data set covering January 1987 to December 2016. This is a viable performance metric when one is interested in measuring prediction accuracy over all periods as a whole, but does not tell us how well an investor would have done *on average over time*. Secondly, asset returns are known to exhibit non-Gaussian characteristics (Cont, 2001). Our analysis of stock returns (Table 2) largely confirms a data set that is potentially impacted by outliers. Therefore, we provide two additional metrics. First, average monthly Spearman’s rank correlation as a non-parameteric measure that does not depend on variance of dependent variable,

$$\bar{\rho}_s = \frac{1}{T} \sum_{t=1}^T \rho(\text{rank}(\mathbf{r}_t), \text{rank}(\hat{\mathbf{r}}_t)).$$

This is also the primary performance metric in Abe and Nakayama (2018). Second, average monthly R^2 as a more conventional complement to R^2_{oos} .

5.2 Simulation results

In this section, we demonstrate the use case of our method. Our synthetic data requires the network to adapt to time-varying dynamics. Table 3 records results

Table 2: Descriptive statistics of monthly excess returns of U.S. equities over April 1957 to December 2016. Monthly excess returns appear to contain some outliers, particularly on the positive end.

	%
Mean	0.70
Std Dev	17.27
Skew	6.739986
Kurtosis	352.81824
Min	-99.90
1%	-38.70
10%	-15.00
25%	-6.51
50%	-0.32
75%	6.24
90%	15.86
99%	54.77
Max	2399.66

of the simulation. As expected, DNN struggled to learn the non-stationary relationships, with mean R^2 of -8.26% and mean rank correlation of -4.07% . OES significantly outperformed the other two methods in this simple simulation, achieving mean R^2 of 49.64% and mean rank correlation of 69.63% . There is a preference for higher L_1 regularization and learning rate. In Aydore et al. (2019), the authors reported problems of exploding gradient with the original method in Hazan et al. (2017) and that DTS-SGD provided greater stability. In our simulation test, we observed gradient instability with DTS-SGD as well. During training, loss can increase after a weight update. This could be an issue with this general class of optimizers. Lastly, we find that mean R^2 tends to be slightly lower than R^2_{oos} .

5.3 Predicting U.S. stock returns

Next, we compare our results against results in Gu et al. (2019), keeping in mind that our method should be compared against DNN without interaction terms. DTS-SGD did not complete training with a reasonable range of hyperparameters due to exploding gradient and was omitted from this section. As an overarching comment, R^2 for both DNN and OES on U.S. stock returns are very low. In our replication (Table 4, without interactions), DNN achieved R^2_{oos} of 0.22% and

Table 3: Simulation results. We observed gradient instability with DTS-SGD which may have contributed to its underperformance.

%	DNN	OES	DTS-SGD
Metrics			
Pooled R^2_{oos}	-7.63	50.21	0.21
Mean R^2	-8.26	49.64	-0.25
Mean Rank Correlation	-4.07	69.63	5.38
Hyperparameters			
Mean L_1	0.01	0.07	0.05
Mean learning rate	0.55	1.00	0.10
Mean W (periods)			16.5
Mean α			86.00

OES achieved -2.51% . However, OES performed substantially better on mean rank correlation, a non-parametric measure, at 4.68% while DNN scored 2.44% . We observed similar performance with or without interaction terms, suggesting that the 8 macroeconomic time series have little interaction effect with the 94 features. In the subsequent results in this section, we only report statistics without interaction terms.

So why do the two metrics diverge? The answer lies in Table 5 and Figure 3. In here, we form decile portfolios based on predicted returns over next month and track their respective realized returns. OES predicted values appear to span a wider range than DNN, this may have contributed to a lower R^2 . DNN used a pooled data set which will average out time-varying effects. As a result, the average gradient will likely be smoother. This is evident from the lower mean L_1 penalty and higher learning rate chosen by validation. By contrast, OES trains on each period individually and the norm of the gradient presented to the network at each period is likely to be larger. This led to lower learning rate and higher mean L_1 penalty chosen by validation. Hence, variance of OES predicted values is higher and may require a higher level of regularization.

In Table 5 and Figure 3, we observe that the prediction performance of DNN is concentrated on the extremities, namely P1 and P10, with realized mean returns of -0.58% and 1.91% respectively. Stocks between P3 and P7 are not well separated. By contrast, OES was better at ranking stocks across the entire spectrum. Realized mean returns of OES are more evenly spread across the deciles, resulting in mean ranked correlation that is almost twice as high as DNN. For the case of an investor iteratively making portfolio allocation decisions, this also reinforces our argument

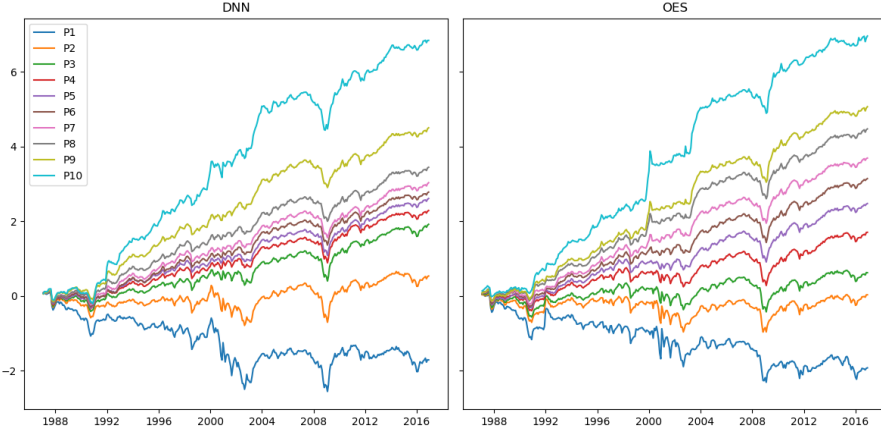
Table 4: Predictive performance on U.S. equities. DNN outperforms OES on R^2 metrics which depend on variance of predicted values but underperformed OES on rank correlation which is non-parametric. Performance was similar with or without interactions terms. Mean hyperparameters are calculated over 10 ensemble networks and across all periods. *As reported* are results in Gu et al. (2019).

%	As reported	With Interactions		W/O Interactions	
		DNN	OES	DNN	OES
Metrics					
Pooled R^2_{oos}	0.4	0.22	-1.93	0.22	-2.51
Mean R^2		-9.40	-11.93	-9.68	-12.17
Mean rank corr		2.89	4.22	2.44	4.69
Hyperparameters					
Mean L_1		0.0012	0.0154	0.0024	0.0064
Mean learning rate		0.77	0.10	0.67	0.10

Table 5: Predicted and realized mean returns by decile where each row represents a decile. $P10-1$ is mean returns of P10 less P1 and shows the return spread between the best predicted stocks relative to the worst predicted stocks. *As reported* are original results from Table A.9 in Gu et al. (2019).

%	As reported		DNN		OES	
	Predicted	Realized	Predicted	Realized	Predicted	Realized
P1	-0.31	-0.92	-0.60	-0.58	-3.47	-0.59
P2	0.22	0.16	0.09	0.08	-1.89	-0.06
P3	0.45	0.44	0.37	0.49	-1.01	0.12
P4	0.60	0.66	0.55	0.60	-0.32	0.42
P5	0.73	0.77	0.70	0.69	0.26	0.64
P6	0.85	0.81	0.85	0.75	0.79	0.84
P7	0.97	0.86	1.00	0.82	1.33	1.00
P8	1.12	0.93	1.18	0.94	1.94	1.23
P9	1.38	1.18	1.43	1.24	2.75	1.40
P10	2.28	2.35	2.31	1.91	4.18	1.96
P10-1	2.58	3.27	2.91	2.48	7.65	2.55

Figure 3: Cumulative mean returns by decile sorted based on predictions by DNN and OES. PN indicates Decile N . High N portfolios (i.e., P10) should be higher and low N portfolios (i.e., P1) should be lower.



that R^2 may not be the best performance metric.

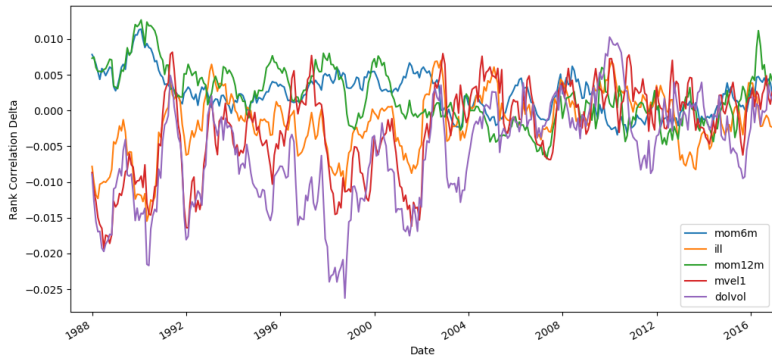
5.4 Time-varying feature importance

So far, our tests are predicated on time-varying relationships between features and stock returns. How do features' importance change over time? To illustrate, at every month we train the OES model and make a prediction. Rank correlation for the baseline model is calculated, then each feature is iteratively set to zero and rank correlation is calculated again. Feature importance of the j -th feature is measured as $\rho_{baseline} - \rho_j$. Note that a feature can have negative importance. For instance, sum of importance for 1 month price momentum is strongly negative, indicating the network was betting on short term reversal. This exercise is different to Section 3.3 in Gu et al. (2019), where a feature is set to zero before training, meaning the network can learn a different model to the baseline. Instead, our method measures what has been learned by the network.

First, we track feature importance over January 1987 to December 1991. The top 10 features with the highest *absolute average delta* were (in order of decreasing importance): *dolvol* (monthly traded value), *mvel1* (log market capitalization), *mom12m* (12-month minus 1-month price momentum), *ill* (illiquidity), *mom6m* (6-month minus 1-month month price momentum), *idiovol* (CAPM residual volatility), *std_dolvol* (36-month traded value volatility), *maxret* (30-day max daily return), *turn* (turnover), and *betasq* (CAPM beta squared). Rolling 12-month averages were calculated to provide a more discernible trend, as illustrated

in Figure 4. Feature importance exhibits strong non-stationarity. Average rank correlation delta can transit between positive and negative, indicating potential for periods of poor performance had an investor naively invested with a style, i.e., always invest *with* momentum. Features such as *dolvol* had trended towards zero over time, indicating loss of explanatory power.

Figure 4: Top 5 features based on rolling 12-month average rank correlation delta to baseline over 1987-1991. *ill*, *mvel1* and *dolvol* have distinctly time-varying importance and have drifted towards zero over time, suggesting loss of explanatory power.



Next, we divide the out-of-sample period into six 5-year blocks and examine change in importance for all features. Figure 5 records that a small set of features contributed most of the efficacy and the set of best features can change over time. For instance, the size effect (*mvel1*) has diminished over time, consistent with literature (i.e., Horowitz et al. 2000). This underscores the importance to have a dynamic model that adapts to changes in the true model.

5.5 Training Deeper Networks

Gu et al. (2019) documents that shallow networks outperformed deeper networks. The authors found that performance peaked at three hidden layers for a neural network and tree-based algorithms tend to select trees with fewer leaves. The authors attributed this tendency for a compact model to relatively small amount of data and low signal-to-noise ratio.

We confirm that performance peaks at three hidden layers. Table 6 records performance metrics of both DNN and OES with three, four and five hidden layers,

Figure 5: Average rank correlation delta to baseline (in decimal) in 5-year blocks. The OES network appeared to only use a handful of features. Some features appear to have lost their importance over time (i.e., *dolvol*, *maxret*, *mom12m* and *mvel1*).

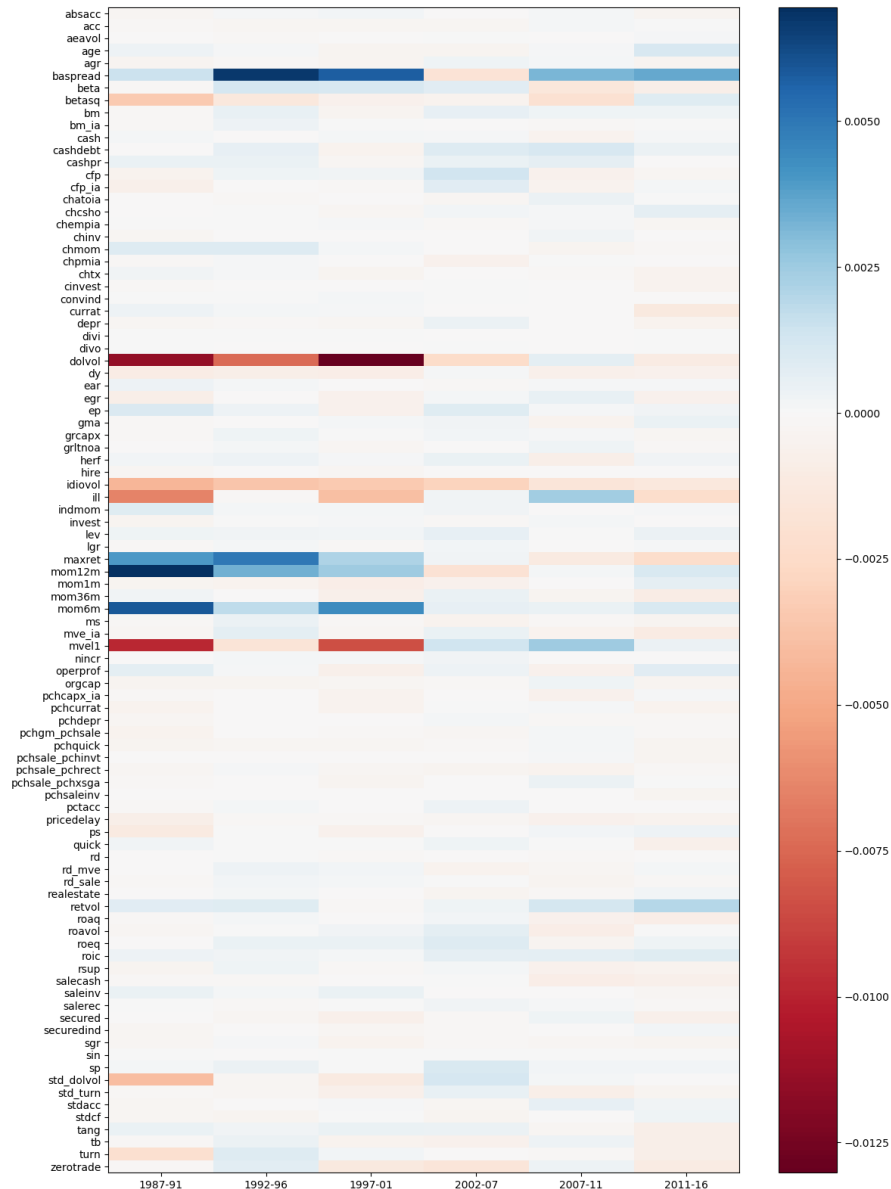
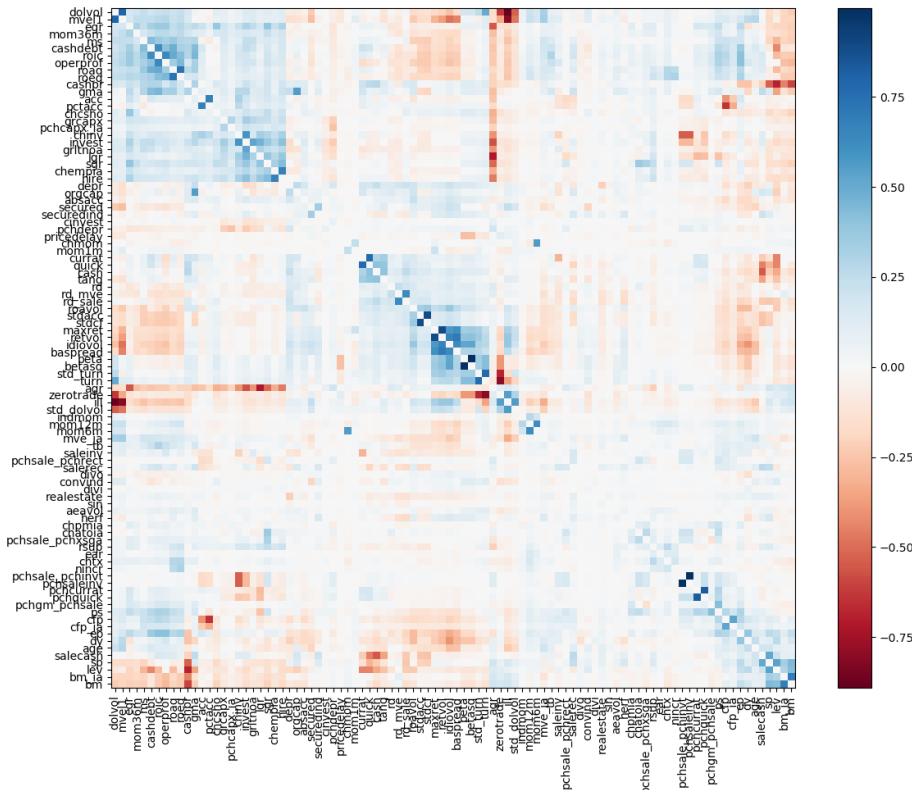


Table 6: Predictive performance on U.S. equities using different network topologies. 3 hidden layers has 32–16–8 nodes, 4-layers has 64–32–16–8, and 5-layers has 128–64–32–16–8.

	DNN			OES		
	3	4	5	3	4	5
Hidden layers						
Metrics (%)						
Pooled R^2_{oos}	0.22	0.21	0.20	-2.51	-2.73	-2.53
Mean R^2	-9.68	-9.69	-9.63	-12.17	-12.38	-12.11
Mean rank correlation	2.44	1.98	1.96	4.69	4.35	4.02

Figure 6: Cross-correlation of all features, calculated each month then average over all time periods. Features are then clustered using correlation as a distance measure. Diagonal of the matrix has been set to zero. Groups of related features are visible in the data set.



with each layer expanding by the pyramid rule. Mean rank correlation peaks at 2.44 % for DNN and falls to 1.96 % at five layers, while OES peaks at 4.69 % and falls to 4.02 %. However, we offer an alternative explanation for the lack of improvement with deeper networks. As observed in Figure 5, only a small subset of features contribute to the network’s performance. The feature set contains many features that are related. For instance, both 6- and 12-month momentum scores are present, as well as return on equity, assets and invested capital. An inspection of cross-correlation confirms our hypothesis. For every month, we construct cross-correlation matrix of all features, then average of the correlation matrix over time. Clustering was applied using $1 - \rho_{i,j}$ as the distance measure, where $\rho_{i,j}$ is rank correlation between feature in row i and column j in the matrix. The resultant correlation matrix is shown in Figure 6. The correlation matrix is suggestive of three broad families of features, as well as many features that do not fit in a family. One in the top left corner, consisting of size, liquidity and profitability. A second group in the middle consisting of volatility, and accounting measures of liquidity (cash and quick ratios). And a third group in the bottom right corner consisting of yield metrics. The *effective feature set* is likely to be smaller than the 94 features listed. Another point to note is the use of L_1 regularization which encourages a sparse network and could explain the low feature utilization.

6 Conclusions

Stock return prediction is an arduous task. The true model is noisy, complex and time-varying. Mainstream deep learning research has focused on problems that are stationary and, arguably, non-stationary applications have seen less advancements. In this work, we introduced an online early stopping algorithm that is easy to implement and can be applied to an existing network setup. We show that a network trained with OES can track a non-stationary function and achieved superior performance to DTS-SGD, a recently proposed online optimization technique. Our method is also significantly faster, as only two periods of training data are required at each iteration, compared to the pooled method used in Gu et al. (2019) which re-trains the network on the entire data set annually. In our tests, the pooled method took 5.5 hours to iterate through the entire data set (an ensemble of ten networks therefore takes 55 hours)⁹. By contrast, our method took 44.25 mins for a single pass over the entire data set (an ensemble of ten networks took 7.4 hours).

Gu et al. (2019) suggested that a small data set and low signal-to-noise ratio were reasons for the lack of improvement with a deeper network. To this end,

⁹Tests performed on AMD Ryzen 7 3700X, 64GB memory, Python 3.7.3, Tensorflow 1.12.0 and Keras 2.2.4. Hyperparameter grid search was performed concurrently.

we showed that only a handful of features contributed to prediction performance. This may be due to correlation between features and the use of L_1 regularization which encourages sparsity. We have also found evidence of time-varying feature importance. In particular, features such as log market capitalization and 12-month minus 1-month momentum appear to have lost their importance towards the end of our test period — a result which will have strong implications for practitioners forecasting stock returns using known asset pricing anomalies. Lastly, we believe time-varying neural network is a relatively less explored domain of machine learning that has many potential applications and deserves further research.

References

Abe, M. and Nakayama, H. (2018). Deep learning for forecasting stock returns in the cross-section.

Aydore, S., Zhu, T., and Foster, D. P. (2019). Dynamic local regret for non-convex online forecasting. In Wallach, H., Larochelle, H., Beygelzimer, A., d’Alché Buc, F., Fox, E., and Garnett, R., editors, *Advances in Neural Information Processing Systems 32*, pages 7980–7989. Curran Associates, Inc.

Bergmeir, C., Hyndman, R., and Koo, B. (2018). A note on the validity of cross-validation for evaluating autoregressive time series prediction. *Computational Statistics & Data Analysis*, 120:70–83.

Bossaerts, P. and Hillion, P. (1999). Implementing statistical criteria to select return forecasting models: What do we learn? *The Review of Financial Studies*, 12(2):405–428.

Cont, R. (2001). Empirical properties of asset returns: stylized facts and statistical issues. *Quantitative Finance*, 1:223–236.

Foster, D. P. and Vohra, R. V. (1998). Asymptotic calibration. *Biometrika*, 85(2):379–390.

Gama, J. a., Žliobaité, I., Bifet, A., Pechenizkiy, M., and Bouchachia, A. (2014). A survey on concept drift adaptation. *ACM Computing Surveys*, 46(4):44:1–44:37.

Goodfellow, I., Bengio, Y., and Courville, A. (2016). *Deep Learning*. MIT Press. <http://www.deeplearningbook.org>.

Gu, S., Kelly, B. T., and Xiu, D. (2019). Empirical asset pricing via machine learning. *Review of Financial Studies*, forthcoming.

Hazan, E., Singh, K., and Zhang, C. (2017). Efficient regret minimization in non-convex games. In Precup, D. and Teh, Y. W., editors, *Proceedings of the 34th International Conference on Machine Learning*, volume 70 of *Proceedings of Machine Learning Research*, pages 1433–1441, International Convention Centre, Sydney, Australia. PMLR.

Horowitz, J. L., Loughran, T., and Savin, N. (2000). The disappearing size effect. *Research in Economics*, 54(1):83–100.

Ioffe, S. and Szegedy, C. (2015). Batch normalization: Accelerating deep network training by reducing internal covariate shift. In *Proceedings of the 32nd International Conference on International Conference on Machine Learning*, volume 37 of *ICML’15*, pages 448–456. JMLR.org.

Kalai, A. and Vempala, S. (2005). Efficient algorithms for online decision problems. *Journal of Computer and System Sciences*, 71(3):291–307.

Kingma, D. P. and Ba, J. (2015). Adam: A method for stochastic optimization. In *International Conference on Learning Representations*, pages 1–13.

Mahsereci, M., Balles, L., Lassner, C., and Hennig, P. (2017). Early stopping without a validation set. *CoRR*, abs/1703.09580.

Messmer, M. (2017). Deep learning and the cross-section of expected returns. Working Paper.

Morgan, N. and Bourlard, H. A. (1990). Generalization and parameter estimation in feedforward nets: Some experiments. In Touretzky, D. S., editor, *Advances in Neural Information Processing Systems 2*, pages 630–637. Morgan-Kaufmann.

Pesaran, M. H. and Timmermann, A. (1995). Predictability of stock returns: Robustness and economic significance. *Journal of Finance*, 50:1201–1228.

Prechelt, L. (1998). Early stopping - but when? In *Neural Networks: Tricks of the Trade, This Book is an Outgrowth of a 1996 NIPS Workshop*, pages 55–69, London, UK, UK. Springer-Verlag.

Reed, R. D. (1993). Pruning algorithms-a survey. *Transactions on Neural Networks*, 4(5):740–747.

Rossi, B. and Inoue, A. (2012). Out-of-sample forecast tests robust to the choice of window size. *Journal of Business & Economic Statistics*, 30(3):432–453.

Schroff, F., Kalenichenko, D., and Philbin, J. (2015). Facenet: A unified embedding for face recognition and clustering. In *2015 IEEE Conference on Computer Vision and Pattern Recognition (CVPR)*, pages 815–823.

Shalev-Shwartz, S. (2012). Online learning and online convex optimization. *Foundations and Trends in Machine Learning*, 4(2):107–194.

Sjberg, J. and Ljung, L. (1995). Overtraining, regularization and searching for a minimum, with application to neural networks. *International Journal of Control*, 62(6):1391–1407.

Srivastava, N., Hinton, G., Krizhevsky, A., Sutskever, I., and Salakhutdinov, R. (2014). Dropout: A simple way to prevent neural networks from overfitting. *Journal of Machine Learning Research*, 15(1):1929–1958.

Sutskever, I., Martens, J., Dahl, G., and Hinton, G. (2013). On the importance of initialization and momentum in deep learning. In Dasgupta, S. and McAllester, D., editors, *Proceedings of the 30th International Conference on Machine Learning*, volume 28 of *Proceedings of Machine Learning Research*, pages 1139–1147, Atlanta, Georgia, USA. PMLR.

Sutskever, I., Vinyals, O., and Le, Q. V. (2014). Sequence to sequence learning with neural networks. In *NIPS*.

Weigand, A. (2019). Machine learning in empirical asset pricing. *Financial Markets and Portfolio Management*, 33:93–104.

Yang, T., Zhang, L., Jin, R., and Yi, J. (2016). Tracking slowly moving clairvoyant: Optimal dynamic regret of online learning with true and noisy gradient. In *Proceedings of the 33rd International Conference on International Conference on Machine Learning - Volume 48*, ICML’16, pages 449–457. JMLR.org.